Cerebral Cortex October 2013;23:2337–2346
doi:10.1093/cercor/bhs233
Advance Access publication August 8, 2012

Neural Mechanisms of Age-Related Slowing: The $\Delta CBF/\Delta CMRO_2$ Ratio Mediates Age-Differences in BOLD Signal and Human Performance

Joanna L. Hutchison[1,2], Hanzhang Lu[3] and Bart Rypma[1,2]

[1]School of Behavioral and Brain Sciences, University of Texas at Dallas, Richardson, TX 75080, USA, [2]Department of Psychiatry, University of Texas Southwestern Medical Center, Dallas, TX 75390, USA and [3]Advanced Imaging Research Center and Department of Radiology, University of Texas Southwestern Medical Center, Dallas, TX 75390, USA

Address correspondence to J.L. Hutchison, Center for Brain Health, University of Texas at Dallas, 2200 W. Mockingbird Lane, Dallas, TX 75235, USA. Email: joanna.hutchison@utdallas.edu.

The precise mechanisms that give rise to the blood-oxygen-level-dependent (BOLD) activation differences that accompany age-related cognitive slowing remain fundamentally unknown. We sought to isolate the origin of age-related BOLD changes by comparing blood-flow and oxygen-metabolic constituents of the BOLD response using dual-echo arterial spin labeling during visual stimulation and CO_2 ingestion. We hypothesized, and our results confirmed, that age-related changes in the ratio of fractional cerebral blood flow to fractional cerebral metabolic rate of oxygen consumption ($\Delta CBF/\Delta CMRO_2$) lead to the BOLD changes that are observed in older adults. $\Delta CBF/\Delta CMRO_2$ was also significantly related to performance, suggesting that age-related cognitive slowing results from neural cell assemblies that operate less efficiently, requiring greater oxygen metabolism that is not matched by blood-flow changes relative to younger adults. Age-related changes in $\Delta CBF/\Delta CMRO_2$ are sufficient to explain variations in BOLD responding and performance cited throughout the literature, assuming no bias based on physiological baseline $CMRO_2$.

Keywords: aging, BOLD, CBF, $CMRO_2$, dual-echo ASL, hypercapnia, neural efficiency, processing efficiency

Introduction

Observations of age-associated performance declines have led to hypotheses suggesting that these declines are governed by reductions in fundamental resources (Hasher and Zacks 1988; Salthouse 1996). In particular, processing efficiency deficits have been implicated in slower reaction times (RTs) observed in older individuals across a variety of paradigms, ranging from visual tasks (Welford 1981; Speranza et al. 2001) to working memory tasks (Anders et al. 1972; Craik and Jennings 1992; Rypma et al. 2005).

Attempts to find indices of age-related resource decline have extended to age-group comparisons of blood-oxygen-level-dependent (BOLD) activity, as measured by the hemodynamic response function (HRF, the function that describes relationships between neural and vascular activity over time; Gössl et al. 2001) using functional magnetic resonance imaging (fMRI). Age-related increases and decreases in BOLD activity (Grady 2002; Hedden and Gabrieli 2004; Rajah and D'Esposito 2005; Nyberg and Bäckman 2011) are often interpreted as aging effects upon neural activity and form the basis for current neurocognitive aging hypotheses (Cabeza 2002; Park et al. 2002; Reuter-Lorenz and Cappell 2008). Neural activity, however, is but one among a set of factors from which the BOLD response arises (Hoge et al. 1999a) that could change with age and lead to age-related BOLD differences (Moeller et al. 1996; Davis et al. 1998; Hoge et al. 1999a; Rypma and D'Esposito 2000, 2001; D'Esposito et al. 2003; Iadecola 2004; Rypma et al. 2005; Leontiev et al. 2007; Restom et al. 2007; Ances et al. 2009; Motes et al. 2010). The HRF depends upon the integrity of numerous structures and physiological processes that change with age (such as cerebral blood flow [CBF]; D'Esposito et al. 2003; Buxton et al. 2004) and that remain poorly understood. For instance, age-related changes in cerebral vasculature have been observed that could potentially adversely affect accurate measurement of neural activity with BOLD signal (D'Esposito et al. 1999; D'Esposito et al. 2003) and its relationship to behavior.

The BOLD signal, in part, arises when synaptic activity triggers astrocytic control of vasodilating prostaglandins (Rossi 2006; Takano et al. 2006) that mediate CBF, in response to cerebral metabolic rate of oxygen ($CMRO_2$) changes associated with neural activity (Davis et al. 1998; Hoge et al. 1999a, b; Hyder et al. 2001, 2002; Leontiev and Buxton 2007; Fig. 1; see Cauli and Hamel 2010 for review). Thus, cerebral activity leads to fractional increases in cerebral perfusion of oxygenated blood (ΔCBF) that exceed fractional increases in oxygen metabolic rate ($\Delta CMRO_2$) for active neurons, leading to increases in the T2* magnetic resonance (MR) signal known as the BOLD response (Ogawa and Lee 1990; Ogawa et al. 1992). Because ΔCBF and $\Delta CMRO_2$ vary independently, the $\Delta CBF/\Delta CMRO_2$ ratio can differ substantially across cortex and influence regional variation in the BOLD response. Few studies have extended this knowledge to hypotheses of age-related variation in BOLD activity and behavior (Mohtasib et al. 2012). We hypothesized that age-related changes in the performance are related to changes in the $\Delta CBF/\Delta CMRO_2$ ratio. Our study is the first to focus on these basic relationships within visual cortex, minimizing the complexities of strategic effects on functional activity.

Taken separately, ΔCBF and $\Delta CMRO_2$ might partially account for the wide range of age-related fMRI results reported in the literature. However, because age-related changes in ΔCBF and $\Delta CMRO_2$ are heterogeneous across cortex and tasks, age differences in the BOLD response could be differentially affected by fluctuations in one or both of these factors (Buxton et al. 2004). Taken together, the ratio of ΔCBF to $\Delta CMRO_2$ is relatively stable (Leontiev and Buxton 2007) and allows for the heterogeneity of changes in both factors and therefore can potentially account for the region- and task-specific nature of BOLD age differences, and their relationships to performance, that have been documented across cortex. Therefore, we took the novel step of evaluating whether age-related $\Delta CBF/\Delta CMRO_2$ differences, and differences in components of this

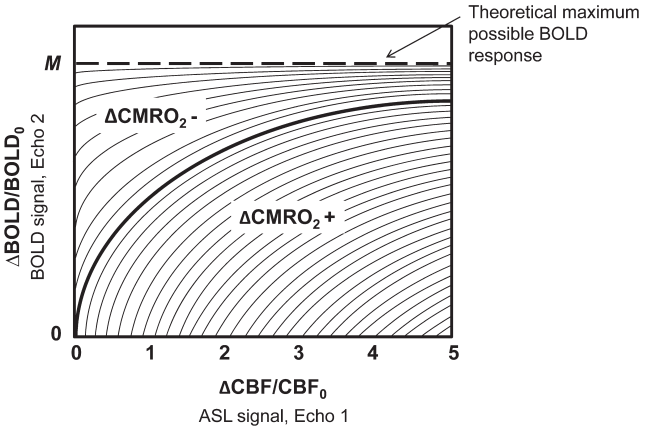

Figure 1. The complex relationship between ΔCBF, $\Delta CMRO_2$, *M*, and BOLD. Age-related changes in ΔCBF and $\Delta CMRO_2$, and the ratio between these physiological processes, can yield age-equivalence or age-difference in the BOLD response. For a given level of ΔCBF, increases in $\Delta CMRO_2$ lead to decreases in the BOLD response (region $\Delta CMRO_2+$). Likewise, decreases in $\Delta CMRO_2$ lead to increases in the BOLD response (region $\Delta CMRO_2-$). Each point along an iso-$\Delta CMRO_2$ contour represents a unique $\Delta CBF/\Delta CMRO_2$ ratio. (Figure from Hoge et al. 1999a, with permission.)

ratio, lead to age-related differences in the BOLD response and behavior. Note that whereas $\Delta CBF/\Delta CMRO_2$ is a key component of the BOLD response, $\Delta CBF/\Delta CMRO_2$ and BOLD are not equivalent due to factors such as *M* (a calibration factor; Davis et al. 1998) that can vary across cortex, participants, and time (cf. Leontiev and Buxton 2007). It has been demonstrated to a certainty that, in intact systems (i.e. in healthy, young participants), increases in $\Delta CBF/\Delta CMRO_2$ lead to increases in BOLD (cf. Fig. 1; e.g. Hoge et al. 1999a; Stefanovic et al. 2004; Leontiev and Buxton 2007; Leontiev et al. 2007). Our hypothesis was that the relationship between ΔCBF and $\Delta CMRO_2$ is fundamentally altered by the process of aging such that the BOLD response might differentially index neural activity in older compared with younger individuals.

To empirically evaluate the role of the $\Delta CBF/\Delta CMRO_2$ ratio in age-related BOLD differences and its relationship to performance, we utilized calibrated fMRI technology to assess visual cortex response to flickering annuli (Welford 1981; Hoge et al. 1999a, b; Pasley et al. 2007; Ances et al. 2009). In the "fixation" condition, BOLD activity generated in response to flickering annuli was compared with that generated during presentation of a fixation cross on a gray background. In the "parafoveal stimulation" condition, a competing stimulus known to inhibit visual cortex was presented prior to the stimulating annulus. During stimulus presentation, participants were required to press response buttons when they noticed a change in the luminance of a central fixation cross (see Fig. 2*B*; Pasley et al. 2007).

To determine individual subjects' theoretical maximum BOLD response in the absence of deoxyhemoglobin *(M*; Davis et al. 1998; Hoge et al. 1999a), we performed a separate hypercapnia scan during which subjects ingested room air and carbon dioxide (CO_2) during 2 sequential time blocks. Hypercapnia induces vasodilation, an increase in venous oxygenation, and a washout of deoxyhemoglobin, which allows for the derivation of *M*. We were then able to calculate $\Delta CMRO_2$ and $\Delta CBF/\Delta CMRO_2$ (Leontiev and Buxton 2007; Leontiev et al. 2007) from resting and parafoveal stimulation conditions for each individual. Some results have suggested that the CBF and BOLD (echo 1 and echo 2, responses, respectively) in calibrated fMRI do not have the same signal-to-noise ratio (Wong et al. 2000), potentially affecting the calculation of $\Delta CMRO_2$. Collection of hypercapnic (Davis et al. 1998) or hyperoxic (Chiarelli et al. 2007) data in tandem with calibrated fMRI ameliorates this concern to the extent that it allows for scaling of the BOLD response to account for differences in the signal-to-noise ratio. Previous work has shown the components of calibrated fMRI to be complementary to one another in elucidating the relationship between vasculature, neural activation, and the BOLD response (see Brown et al. 2007).

Our results showed that age-related increases in $\Delta CMRO_2$ led to significant age decrements in the $\Delta CBF/\Delta CMRO_2$ ratio and thus a lower BOLD signal for older adults. These results support the hypothesis that age-related BOLD changes are mediated by changes in $\Delta CBF/\Delta CMRO_2$. Further, a significant relationship between changes in $\Delta CBF/\Delta CMRO_2$ and performance suggests that age-related $\Delta CBF/\Delta CMRO_2$ changes observed at the physiological level play a central role in age-related processing efficiency reductions observed at the behavioral level.

Materials and Methods

Participants

Twenty-two healthy younger (age: 23–33, mean age: 28.2 years; $n = 11$, 6 females) and older (age: 53–72, mean age: 60.5 years; $n = 11$, 6 females) individuals participated. Recruits came from the web, from advertisements in circulars and flyers distributed throughout the Dallas-Fort Worth Metroplex, and from the University of Texas at Dallas (UTD) and the University of Texas Southwestern Medical Center (UTSWMC) campuses. All advertisements were approved by the UTSWMC and UTD Institutional Review Boards (IRBs).

No participants were taking blood pressure medications, diuretics, or psychotropic/psychoactive medications, and none reported any history of heart, lung, neurological, or psychiatric difficulties. All participants were screened and deemed safe within the 3 Tesla (3T) MR scanning environment. Participants were also cognitively intact based on assessments during the telephone prescreening (de Jager et al. 2003) and in person on the day of the scans (Folstein et al. 1975). Participants were compensated at the rate of $100 for their time (~$50 per hour, including time to consent using a form approved by both the UTSWMC and UTD IRBs).

Visual Stimuli

Flashing sinusoidal grating annuli were presented to activate or depress activity within cortical regions of interest (ROIs), which were the visual areas corresponding to peripheral visual field (Pasley et al. 2007). Three types of stimuli were presented: Parafoveal, or negative response, stimuli (1.7–3.3° eccentricity, drift temporal frequency = 6 Hz, spatial frequency = 1 cycle per degree, 80% contrast); peripheral, or positive response, stimuli (6.8–9.9° eccentricity, drift temporal frequency = 6 Hz, spatial frequency = 1 cycle per degree, 25% contrast); and combined stimuli (parafoveal stimulus onset followed by peripheral stimulus onset after a 20 s delay, maintaining both images in view simultaneously after positive response stimulus onset). A fixation cross was presented in the center of the screen throughout the visual task. It changed in luminance every 3–7 s, with the mean time between luminance changes equal to 5 s. Stimuli were presented in 3 runs, with 2 instances of each stimulus block per run, randomized in order within each run, and with 30 s fixation periods spaced temporally between blocks, for a total of 6 instances of each stimulus block concatenated across runs. Each run lasted a total of 600 s (i.e. 10 min).

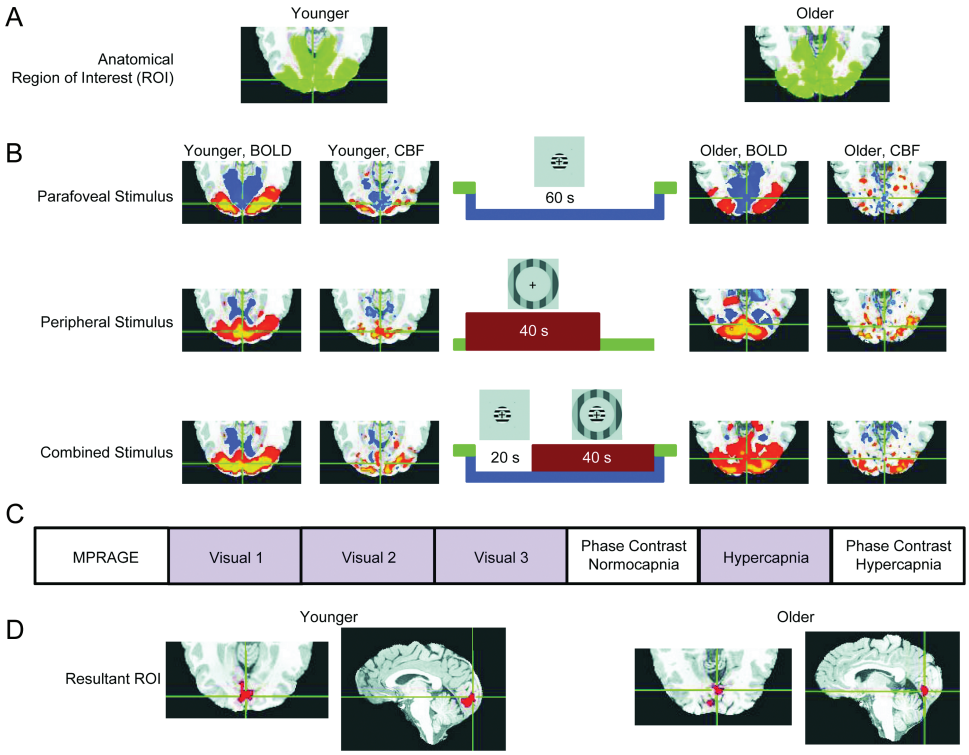

Figure 2. Regions of interest and the experimental paradigm. (*A*) Representative younger and older anatomical regions of interest (ROIs) based on Brodmann areas (BAs) 17, 18, and 19, which encompass visual cortex. (*B*) Representative younger and older responses to visual stimulation (CBF and BOLD) depicted under different stimulus conditions (parafoveal, peripheral, and combined response; axial view, visual cortex; cf. Pasley et al. 2007). Cool colors indicate negative activations compared with fixation; warm colors indicate positive activations compared with fixation, all corrected $P < .05$. The time course of the visual stimulation is shown along with the corresponding stimulus. For the time course, green represents fixation, blue represents parafoveal stimulation, and red represents peripheral stimulation. (*C*) The order of scans. Scans shaded in purple were dual-echo arterial spin labeling (ASL) scans, during which both CBF and BOLD signals were acquired. (*D*) The ROI resulting from the combination of the anatomical ROI and functional activation requirements from the visual task. To be retained in the final ROI, a voxel had to be contained within the anatomical ROI and have a negative response to the parafoveal stimulus but a positive response to both the peripheral and combined stimuli. All statistics were computed on the resultant ROI.

Hypercapnia Materials

A 2-way nonrebreathing valve/mouthpiece combination (Hans Rudolph, 2600 series, Shawnee, KS, United States of America) was used to deliver a 5% CO_2 solution (balanced with 21% O_2 and 74% N_2; contained in a Douglas bag) for hypercapnic induction. A capnograph device (Capnogard, Model 1265, Novametrix Medical Systems, CT, United States of America) was used to monitor end-tidal CO_2, and a pulse oximeter (MEDRAD, Pittsburgh, PA, United States of America) was used to monitor breathing rate, heart rate, and arterial oxygenation saturation. Values from both devices were recorded on a Lenovo tablet PC running the Microsoft Vista operating system and using HyperTerminal (Private Edition, Version 6.3, by Hilgraeve, Monroe, MI, United States of America) for data collection.

Apparatus and Scanning Parameters

All imaging was conducted at the UTSWMC Advanced Imaging Research Center on a 3T MRI system (Philips Medical Systems, Best, The Netherlands). High-resolution anatomical data were acquired using a T1-weighted magnetization-prepared rapid acquisition of gradient echo (MPRAGE) pulse sequence (Brant-Zawadzki et al. 1992). Calibrated fMRI functionally incorporated both arterial spin labeling (ASL; echo 1, dependent on CBF) and BOLD (echo 2, dependent on both CBF and $CMRO_2$). A pseudo-continuous ASL sequence (Garcia et al. 2005) was used to acquire the calibrated fMRI data (visual, hypercapnia) with echo times at TE1 = 11 ms and TE2 = 30 ms (Flip angle = 90°, 16 slices, 5 mm thick, orientation transverse, slice around calcarine sulcus linearly from bottom to top, TR = 4 s, 150 volumes). Global baseline CBF was measured in saggital sinus (phase contrast voxel size 0.45×0.45×5 mm^3, maximum velocity 80 cm/s, duration 30 s; note that hypercapnia-induced CBF increases are comparable for sagittal sinus and feeding arteries, which perfuse the entire brain; Aslan et al. 2010) using phase contrast scans that were run immediately prior to and immediately following the hypercapnia sequence, representing normocapnic and hypercapnic conditions, respectively. Phase contrast MRI data were used to normalize ASL signals as described previously (Aslan et al. 2010). Scans were acquired in the following sequence: High-resolution anatomical MPRAGE, 3 runs of the visual task, normocapnic phase contrast, hypercapnia, and hypercapnic phase contrast (Fig. 2*C*).

Procedure

The high-resolution anatomical MPRAGE was acquired first, followed by 3 runs of the visual task. Participants were asked to ignore the flashing annuli but to quickly press and release both buttons (incorporated into hand-held button boxes) every time they noticed the fixation cross changing in luminance—that is, appearing lighter or darker. This task served to maintain the participants' focus on the center of the screen so that positive response cortical areas could be located functionally using calibrated fMRI.

At the conclusion of the visual stimulus runs, the patient table was withdrawn from the bore of the scanner and the mouthpiece for the hypercapnia portion of the experiment was placed into the participant's mouth. The participant wiped the exterior of his or her nose with a moist towelette, the nose clip was placed on the participant's nose, and it was verified that the participant could breathe comfortably and that the nonrebreathing valve was working properly. Button boxes were removed and a pulse oximeter finger monitor was clipped onto a finger of the participant's left hand. An emergency squeeze bulb was positioned near the right hand such that the participant could easily squeeze it without having to move or look for the

bulb. The patient table was returned to the scanner bore and the hypercapnia experiment procedure was executed, flanked by 2 4-min phase contrast scans (normocapnic and hypercapnic, respectively). A researcher stayed inside the magnet room throughout the phase contrast and hypercapnia portions of the experiment to manually switch the valve to control the breathing of air (either room air or CO_2 bag). At the termination of the final scan, the bag valve was returned to room air, the patient table was withdrawn from the bore of the scanner, and the hypercapnia equipment was removed from the participant.

Data Pre-Processing

Data were taken from Philips PAR/REC format and transformed into SPM (Statistical Parametric Mapping, Wellcome Department of Imaging Neuroscience, University College London, London, United Kingdom) Analyze format using the GUI FOR R2A Rec-to-Analyze Converter (Hermans and Neggers, GUI for R2A, version 2.1 released March 2006, modified February 2008, Helmholtz Institute, Utrecht University, Dept of Brain Research, University Medical Center, Utrecht, Netherlands). Files were then spatially pre-processed in SPM using the Realign-Estimate-Reslice algorithm for each echo and run. In-house MATLAB® (Version 7.4, Mathworks, Natick, MA, United States of America) code separated Echo 1 and Echo 2 into separate Rec files for each echo and run, and the new Rec files were then read into AFNI (Analysis of Functional NeuroImages; Cox 1996) where the data were registered to the individual's MPRAGE space and aligned to the first brick of the first run of Echo 2 (dummy scans prevented the need to discard the first few volumes). Parameters were saved and applied to all runs for both Echo 2 and Echo 1. Labeled images were subtracted from control images in Echo 1 to obtain CBF weighted images. Echo 2 data were subjected to a low pass temporal Fourier filter (0.05) and were then spatially smoothed (FWHM = 8). Noise was cleared from outside the head. A mask was then generated to restrict analyses to areas representing visual cortex—specifically, we utilized a morphometric approximation of Brodmann Areas (BAs; Brodmann 2006/1909) 17, 18, and 19. BAs were defined by the demarcation of landmarks in each individual's native space using Caret (Van Essen et al. 2001); landmarks included those automatically generated by Caret prior to flattening (Medial Wall Dorsal, Medial Wall Ventral, and Calcarine Fissure), those recommended by Caret after flattening (the central sulcus, the Sylvian fissure, and the anterior half of the superior temporal gyrus; Van Essen, 2005), and those found by our laboratory to be consistently identifiable and accurate in deriving cleaner, more accurate BA demarcation across participants, also after flattening (inferior rostral sulcus, Pars Triangularis, Pars Orbitalis, inferior frontal sulcus, and superior temporal sulcus). Native-space landmarks were spherically registered to a Colin-brain template incorporating all BAs, and these BAs were then transformed into each individual's native space (cf. Fig. 2*A*). Functional activation in response to the visual stimuli was used to narrow ROI selection as described below.

Data Analyses, Visual Data

Echo 1 and Echo 2 data, reflecting CBF and BOLD, respectively, were analyzed using 3dDeconvolve to conduct a regression analysis in AFNI (Cox 1996). Beta values, along with their associated *P* values, were generated for each individual for each stimulus condition for each echo.

For further analysis, ROI selection was based on functional activation overlap between CBF and BOLD but was restricted to the morphometrically defined visual cortical areas BAs 17, 18, and 19 (see above). In light of evidence suggesting that the dependent measures of interest might be less prone to bias if blood flow is taken into account and ROIs are sufficiently large (Leontiev et al. 2007), we required overlap of CBF and BOLD activation but selected a generous thresholding measure (Poline et al. 2006) such that *t* values of 1.00 were adequate for positive and negative response conditions, and the combined condition had no statistical thresholding. Thus, in order for a voxel to be retained within the ROI, it had to: 1) react positively to the peripheral stimulus for both CBF and BOLD, 2) react negatively to the parafoveal stimulus for both CBF and BOLD, 3) react positively to the combined stimulus for both CBF and BOLD, and 4) be contained within the morphometrically defined BAs 17, 18, and 19 (cf. Fig. 2*D*). ROIs for individuals ranged from 6 to 269 voxels (younger: 18–269 voxels, mean = 128.7, standard deviation [SD] = 81.7; older: 6–136 voxels, mean = 65.4, SD = 41.3). Concerns regarding biases introduced by ROI size differences between the groups are obviated by our results, which indicate a pattern opposite to previous observations that smaller functional ROIs tend to be associated with larger $\Delta CBF/\Delta CMRO_2$ ratios (Leontiev et al. 2007), and thus typically larger BOLD responses. All results reported here were averaged over the ROI for the stimulus condition of interest unless specifically stated as being calculated over the whole brain.

Beta values from the regression analysis were adjusted to reflect percent signal change from fixation (for echoes 1 and 2, respectively) and were then masked by the ROI selection that included the overlap area between CBF and BOLD activations to obtain mean values per stimulus condition for younger and older groups. Additional statistical analyses were conducted using SAS® software program (Version 9.1, SAS Institute, Cary, NC, United States of America) outside of brain space.

Data Analyses, Hypercapnia Data

Data in Echo 1 were used to obtain CBF weighted images and data in Echo 2 represented the BOLD images, as described above. The ROI masks defined in the visual fMRI runs were applied to the hypercapnia data to obtain time courses of CBF and BOLD signals. The CBF and BOLD percent signal changes were calculated comparing the average hypercapnia signal (volumes 91–150) to the average normocapnia signal (volumes 1–60).

Continuing to use in-house Matlab code, we used the Davis et al. (1998) and Hoge et al. (1999a) model to estimate *M* (a value necessary for the calculation of $CMRO_2$; Davis et al., 1998) from calibrated fMRI hypercapnia data: $M = \text{BOLD percentage}/(1 - (1 + \text{CBF percentage}) \exp(\alpha - \beta))$, with the assumption that $CMRO_2$ and neural activity are not significantly affected by hypercapnic conditions (Hoge et al. 1999b). We assumed α equals 0.38 (Grubb et al. 1974) and β equals 1.33 (Lu and van Zijl 2005); Hoge et al. (1999a) demonstrated that although estimates of α and β affect asymptotic extrapolations of *M*, these values do not significantly impact results in the range of human imaging studies, and so the utilization of estimates for α and β was deemed adequate. *M* was calculated both over the ROI only and over the entire brain. There is some evidence that age-related differences in *M* can lead to differences in the BOLD response (Ances et al. 2009, but see Hoge et al. 1999a). To be thorough, we investigated this possibility and did not find significant differences in *M* values between younger (mean $M = 0.10$, SD = 0.06) and older (mean $M = 0.12$, SD = 0.05) groups, $t(20) = 0.92$, $P = 0.37$,nonsignificant, over the functionally derived ROI; comparing *M* values averaged over the entire brain between the younger and older groups was similarly nonsignificant.

Finally, using *M* from the visually derived ROI, we were able to calculate $\Delta CMRO_2$ and $\Delta CBF/\Delta CMRO_2$ for each individual, both in terms of change from fixation and from parafoveal stimulation. (One younger participant had a $\Delta CBF/\Delta CMRO_2$ ratio exceeding 2.5 SD greater than the remainder of the group. In order to present a clearer picture of the mean group values, this participant's $\Delta CBF/\Delta CMRO_2$ ratio data are not included in the analyses presented in the Results, although the inclusion of this participant's data did not alter the significance of the results.) Similar ratios were calculated for BOLD and CBF data. The Davis et al. (1998) and Hoge et al. (1999a) model was also the basis for these calculations. Because there were no significant differences between groups in their *M* values, we repeated our analyses using the mean *M* for each group (older and younger) and a single mean *M* value that collapsed across both groups. $\Delta CBF/\Delta CMRO_2$ values were still significantly different between the groups. Values reported in the paper use individual *M* values (cf. Chiarelli et al. 2007). $\Delta CBF/\Delta CMRO_2$ was not normally distributed across the sample from either fixation, $W = 0.74$, $P < 0.0001$, or from parafoveal stimulation, $W = 0.81$, $P = 0.0008$. Kruskal–Wallis tests were used to assess group differences under such conditions of nonnormality.

Results

A priori hypotheses of age-related changes in $\Delta CBF/\Delta CMRO_2$ ratios and their relationships to behavior were tested using planned comparisons (cf. Keppel and Wickens 2004). For additional tests we calculated, using false discovery rate (FDR) theory (Benjamini and Hochberg 2000), that we would expect 0.85, or roughly between 0 and 1, of these tests to falsely reject the null hypothesis (0.05*17 = 0.85). For these tests, we rejected the null hypothesis at $P < 0.05$, FDR < 0.05. Thus, it is probable that our tests correctly rejected our null hypotheses, particularly given that the results portray a consistent picture. For the sake of clarity, the FDR is reported in addition to P when $P < 0.05$ and FDR < 0.10.

Behavioral Results

Younger participants (mean RT = 553.93 s, standard error of the mean [SEM] = 31.21) were significantly faster in responding to the fixation-cross luminance change than older participants (mean RT = 677.66 s, SEM = 34.88), $t(20) = -2.86$, $P < 0.01$. Younger participants were also more accurate (mean proportion correct = 0.83, SEM = 0.02) than their older counterparts (mean proportion correct = 0.69, SEM = 0.05), $t(13.5) = 2.61$, $P = 0.02$. There was no evidence of a speed-accuracy trade-off, as RT was negatively associated with proportion correct, Spearman's $\rho = -0.67$, $P = 0.0007$.

Visual Stimulation: BOLD

For the visual experiment (see Fig. 2*B* and *C*), we first sought to test the a priori hypothesis of an age-related difference in the BOLD response, as the etiology of this difference was the topic under study. A general linear model (GLM) incorporating group (younger and older), stimulus conditions of interest (from fixation: Parafoveal, peripheral, and combined; from parafoveal stimulation: combined), and a group by stimulus condition interaction, was significant for determining percent signal change in the BOLD response, $F_{7,80} = 68.93$, $P < 0.0001$, $R^2 = 0.86$. As seen in Figure 3*A*, in addition to differences based on stimulus type, the younger group had a greater BOLD response than the older group, $F_{1,80} = 8.18$, $P = 0.005$.

$\Delta CBF/\Delta CMRO_2$ Ratio

To test the a priori hypothesis that $\Delta CBF/\Delta CMRO_2$ differences could mediate age-related changes in the BOLD response, $\Delta CBF/\Delta CMRO_2$ was calculated for each individual from both resting and parafoveal stimulation conditions (see Fig. 4*A*). $\Delta CBF/\Delta CMRO_2$ was significantly greater for the younger group than the older group, both from fixation (younger: mean = 2.40, SEM = 0.24; older: mean = 1.88, SEM = 0.06), Kruskal–Wallis $\chi^2(1) = 4.17$, $P = 0.04$, and from parafoveal stimulation (younger: mean = 2.00, SEM = 0.12; older: mean = 1.69, SEM = 0.05), $\chi^2(1) = 4.46$, $P = 0.03$ (Fig. 4*B*). These results support the hypothesis that age-related BOLD signal changes are the consequence of differences in the ratio of cerebral perfusion to oxygen metabolic rate (i.e. $\Delta CBF/\Delta CMRO_2$) between the younger and older groups, and these age-related differences occur regardless of baseline stimulation condition (i.e. fixation or parafoveal).

Some studies (e.g. Leontiev et al. 2007) have shown a pattern in which smaller functional ROIs tend to be accompanied by greater $\Delta CBF/\Delta CMRO_2$ ratios. Greater amounts of noise in the data could restrict the ROI size and inflate $\Delta CBF/\Delta CMRO_2$ ratio estimates. If our results were attributable to this ROI size bias, we would expect larger $\Delta CBF/\Delta CMRO_2$ ratios for the older group in comparison to the younger group, and yet we observed the opposite. Moreover, a correlation between percent signal change (CBF and BOLD) and ROI size was not significant ($P = 0.34$ and 0.15, respectively), suggesting that our results do not reflect ROI size differences.

Components of the $\Delta CBF/\Delta CMRO_2$ Ratio

Significant differences in the CBF response would indicate that age-related differences in the BOLD response are at least partially due to blood flow changes that occur with age-related perfusion (i.e. blood flow) changes. As with the BOLD data, we utilized a GLM incorporating group, stimulus conditions of interest (from fixation: Negative, positive, and combined; from parafoveal stimulation: combined), and a group by stimulus condition interaction. The omnibus F statistic indicated that this model was significant for determining percent signal change in the CBF response, $F_{7,80} = 66.42$, $P < 0.0001$, $R^2 = 0.85$. As seen in Figure 3*B*, the CBF difference

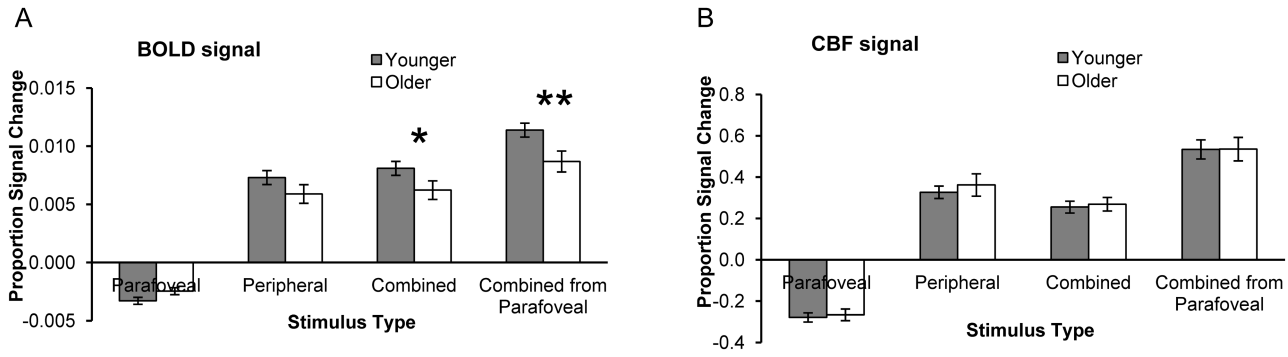

Figure 3. CBF and BOLD responses to visual stimulation. (*A*) BOLD percent signal change (mean ± SEM) for younger and older groups based on visual stimulation shown by stimulus condition. Significant differences between groups are indicated by asterisks: *$P < 0.04$, **$P < 0.004$. (*B*) CBF percent signal change (mean ± SEM) for younger and older groups based on visual stimulation shown by stimulus condition. (Comparison of the combined condition to parafoveal stimulation, shown in the rightmost bars of Fig. 3*A*,*B*, is aggregated from the parafoveal and combined stimulus conditions for both BOLD and CBF—that is, the effects are additive. Although this is not an independent measurement, it is shown here for illustrative purposes).

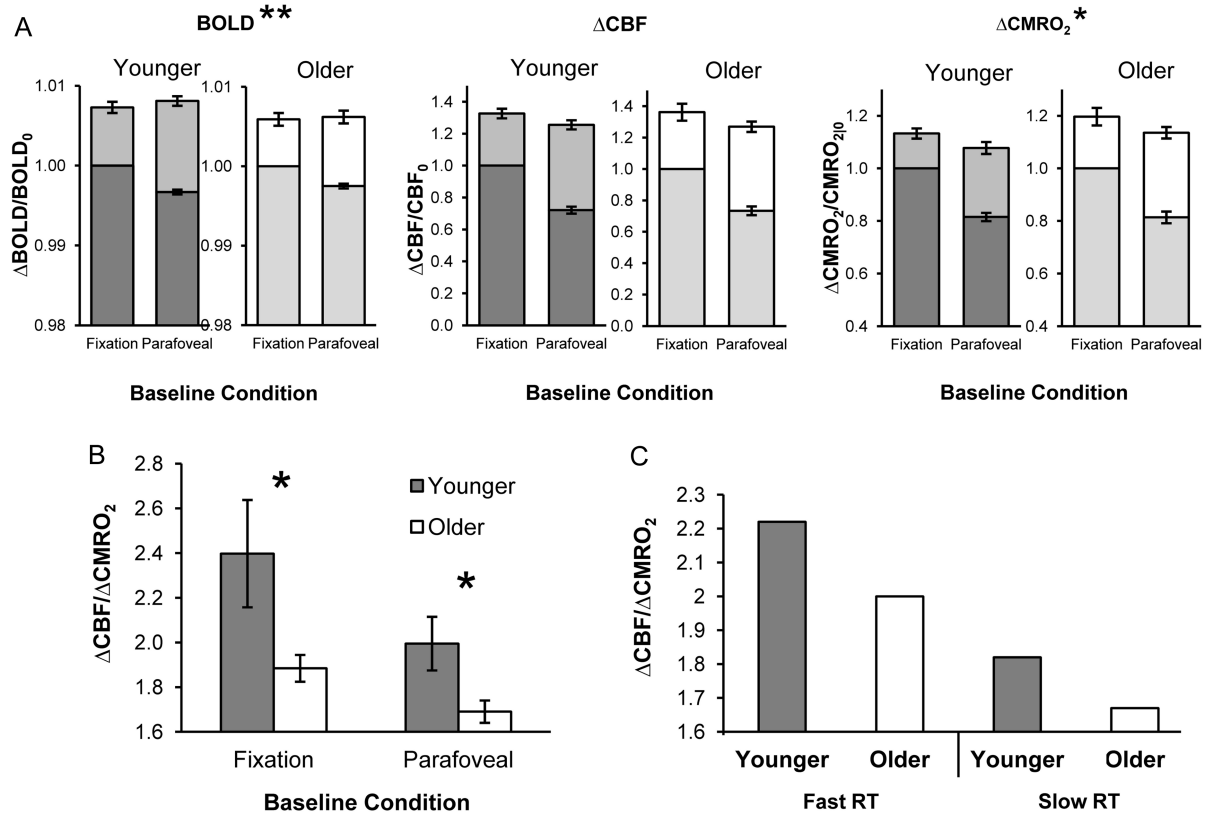

Figure 4. $\Delta CBF/\Delta CMRO_2$ Ratios for Younger and Older Groups. (*A*) Ratios comparing evoked responses (lighter, upper bars) from fixation and parafoveal stimulation conditions (darker, lower bars) for BOLD, ΔCBF, and $\Delta CMRO_2$, normalized to fixation condition levels. Incremental evoked BOLD, ΔCBF, and $\Delta CMRO_2$ responses (mean ± SEM) were greater from parafoveal stimulation than from fixation. Significant differences from fixation between groups are indicated by asterisks: $^*P \leq 0.04$, $^{**}P < 0.004$. (*B*) $\Delta CBF/\Delta CMRO_2$ (mean ± SEM) shown by group membership and condition. Older participants had lower $\Delta CBF/\Delta CMRO_2$ ratios, which were associated with a lower BOLD response. Significant differences between groups are indicated by an asterisk: $^*P \leq 0.04$. (*C*) Younger and older participants were designated as fast or slow responders based on median reaction time (RT) within each group. The resulting median $\Delta CBF/\Delta CMRO_2$ ratios for each group from fixation illustrate the significant association between $\Delta CBF/\Delta CMRO_2$ and RT, which was calculated across groups.

between younger and older groups was not significant, $F_{1,80} = 0.32$, $P = 0.57$, indicating that age-related differences in $\Delta CBF/\Delta CMRO_2$ were not caused by differences in the CBF response. Additionally, there were minimal differences in "absolute" (i.e. change from fixation) CBF in the older compared with the younger group, both from fixation, $\chi^2(1) = 0.24$, $P = 0.62$ (see Fig. 5*A*), and parafoveal stimulation, $\chi^2(1) = 0.05$, $P = 0.82$ (see Fig. 5*B*).

We also sought to determine if there were age-related differences in the $\Delta CMRO_2$ component of $\Delta CBF/\Delta CMRO_2$. We observed age-related $\Delta CMRO_2$ differences in "absolute" measures (i.e. change from fixation; Fig. 5*A*) when measured from parafoveal stimulation, $\chi^2(1) = 4.28$, $P < 0.04$ (Fig. 5*B*; FDR < 0.09). Additionally, we observed greater "incremental" (i.e. change from respective baseline stimulation condition—that is, either fixation or parafoveal stimulation) evoked $\Delta CMRO_2$ from parafoveal stimulation (least squared mean [LSM] = 0.30, SEM = 0.02) than from fixation (LSM = 0.16, SEM = 0.02), $t(21) = 11.17$, $P < 0.0001$; this effect was also found for BOLD and ΔCBF, $P < 0.0001$. However, only the BOLD response showed greater incremental evoked responses for the younger (mean = 0.0094, SEM = 0.0007) than the older group (mean = 0.0073, SEM = 0.0007), $t(20) = 2.09$, $P < 0.05$ (FDR = 0.09), indicating that age-related differences in $\Delta CMRO_2$ are not attributable to baseline stimulation condition differences. In sum, comparing differences between younger and older participants on the constituents of the BOLD response revealed minimal differences in ΔCBF but significant age-related differences in $\Delta CMRO_2$ (Figs 4*C*, 5*A*, *B*). This change in $\Delta CMRO_2$ affected significant change in $\Delta CBF/\Delta CMRO_2$.

$\Delta CBF/\Delta CMRO_2$: Relationships to Behavior

The behavioral significance of age-related $\Delta CBF/\Delta CMRO_2$ differences could be demonstrated if we observed relationships between this physiologic factor and individual subject performance. A Spearman's ρ test of association across younger and older groups confirmed our a priori hypothesis that RT was significantly negatively associated with $\Delta CBF/\Delta CMRO_2$ from fixation, $\rho = -0.49$, $P = 0.02$ (and from parafoveal stimulation, $\rho = -0.43$, $P = 0.05$). Figure 4*C* illustrates this relationship when broken out by group (younger or older) and RT (slower or faster, as determined by within-group median split). Likewise, a Spearman's ρ test of association confirmed our a priori hypothesis that proportion correct was positively associated with $\Delta CBF/\Delta CMRO_2$ from fixation, $\rho = 0.46$, $P < 0.04$. Neither RT nor proportion correct was associated with the ΔCBF or $\Delta CMRO_2$ components separately. These results support the hypothesis that age-related behavioral indices—that is, slowing of RTs and reduced proportion

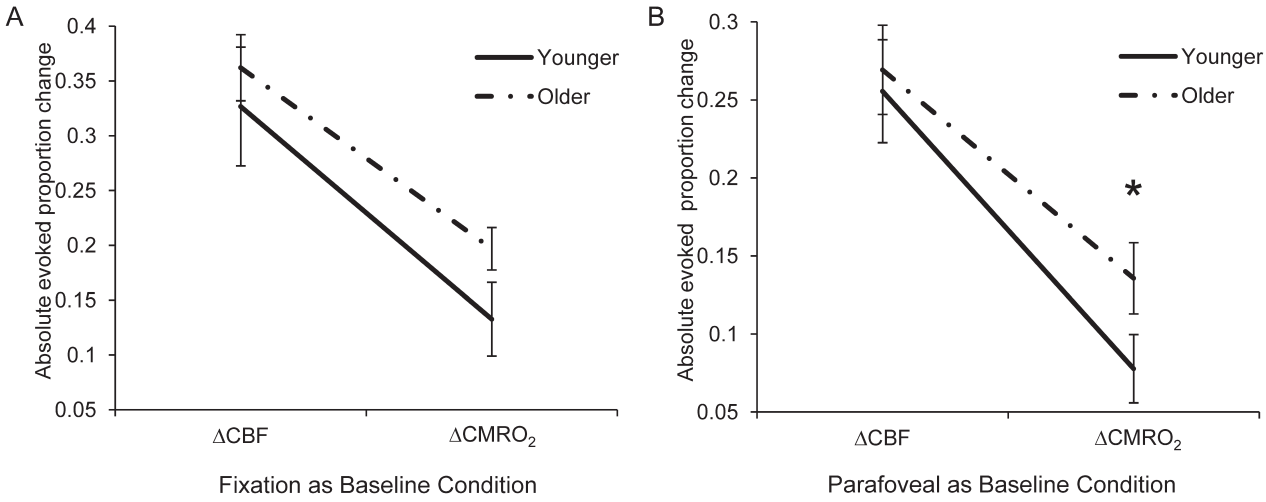

Figure 5. ΔCBF and $\Delta CMRO_2$ evoked responses for younger and older groups. ΔCBF and $\Delta CMRO_2$ evoked responses (mean ± SEM) are shown to compare age-related differences for these constituents of the BOLD response. Data are shown from both (*A*) fixation (ΔCBF: younger mean = 0.33 ± 0.03, older mean = 0.36 ± 0.05; $\Delta CMRO_2$: younger mean = 0.13 ± 0.02, older mean = 0.20 ± 0.03) and (*B*) parafoveal stimulation (ΔCBF: younger mean = 0.26 ± 0.03; older mean = 0.27 ± 0.03; $\Delta CMRO_2$: younger mean = 0.08 ± 0.02, older mean = 0.14 ± 0.02). Significant differences between groups are indicated by an asterisk: *$P \leq 0.04$.

correct—are significantly associated with age-related reductions in $\Delta CBF/\Delta CMRO_2$.

Discussion

Because the ASL signal is dependent on CBF and the BOLD signal is dependent on both CBF and $CMRO_2$, use of dual-echo ASL (i.e. calibrated fMRI) allowed separation of vascular and neural factors and permitted resolution of age-related BOLD signal ambiguities. Our goal was to evaluate whether $\Delta CBF/\Delta CMRO_2$ mediates age-related differences in the BOLD response. The BOLD response was significantly diminished for the older compared with the younger group in visual cortex, whereas ΔCBF responses were equivalent between groups. $\Delta CMRO_2$ was greater in the older group, leading to our observations of reduced $\Delta CBF/\Delta CMRO_2$ for the older group and a reduced BOLD signal to visual flashing annuli, regardless of baseline stimulation condition. Our results implicate a mechanism by which age-related changes in the BOLD response to neural activity arise. They suggest that $\Delta CMRO_2$ increases, not accommodated by ΔCBF increases, lead to reduced fMRI signal in older adults. Further, performance reductions (greater RT and reduced proportion correct in older compared with younger) were significantly associated with reduced $\Delta CBF/\Delta CMRO_2$, suggesting that alterations to $\Delta CBF/\Delta CMRO_2$ affected the processes by which the visual stimuli were perceived.

Conclusions regarding age-equivalent ΔCBF and age-differential $\Delta CMRO_2$ rest on assumptions of linearity between ΔCBF and $\Delta CMRO_2$ and age-equivalent baselines. Several studies suggest linear relationships between ΔCBF and $\Delta CMRO_2$ (e.g. Hoge et al. 1999a, b; Stefanovic et al. 2004) but others do not (e.g. Lin et al. 2010). Age-related increases in $\Delta CMRO_2$ have been observed in some studies assessing different physiological baseline $CMRO_2$ levels between younger and older groups (cf. Hyder et al. 2002). Such baseline differences could influence measured changes in $\Delta CMRO_2$. For example, the elderly might have lower resting values of $CMRO_2$ as suggested by ^{13}C MR spectroscopy (Gjedde 1997; Boumezbeur et al. 2010) and positron emission tomography (e.g. Kety 1956; Marchal et al. 1992). In such a mechanism, the greater $CMRO_2$ change that we observed in the elderly compared with young could reflect activity increases that result in age-equivalent absolute neural activity under stimulation conditions as opposed to a larger neural response (cf. Hyder et al. 2002). Age-differential $CMRO_2$ baseline levels (cf. Hyder et al. 2002) could also influence blood flow response. In such a mechanism, as $CMRO_2$ exceeded resting levels, the fractional increase in CBF needed to supply the increment in oxygen consumption would increase asymptotically as venous pressure of oxygen (pO_2) approached arterial values resulting in increasing $\Delta CBF/\Delta CMRO_2$, as a function of absolute $CMRO_2$ (cf. Buxton and Frank 1997; Lin et al. 2010). In such a mechanism, the increased $\Delta CBF/\Delta CMRO_2$ we observed in younger subjects would reflect their higher resting physiological $CMRO_2$ rather than an alteration in vascular response.

Other research suggests, however, that baseline $CMRO_2$ actually increases with age after accounting for reductions in brain parenchyma volume (Lu et al. 2011). Thus, if age-related $CMRO_2$ baseline changes were driving the age-related differences in $\Delta CMRO_2$ during activation, greater $\Delta CMRO_2$ for younger than for older adults would be expected—the opposite of the result we obtained. Additionally, we measured $\Delta CMRO_2$ from 2 baseline stimulation conditions (i.e. fixation, parafoveal stimulation) to test just such a possibility. Our results showed an increase in $\Delta CMRO_2$ with aging that was greater from parafoveal stimulation than from fixation for both younger and older groups. Although this result does not conclusively demonstrate age-equivalent physiological baselines, it does indicate that $CMRO_2$ increments from different baseline conditions are proportional for both younger and older adults. This result does not support the hypothesis that age-differential $\Delta CMRO_2$ results from age-differential $CMRO_2$ baselines. Future research is certainly needed to clarify the nature of CBF/ $CMRO_2$ linearity and the role of baseline $CMRO_2$ activity in assessing age-related BOLD signal change.

This study focused on activation-induced $\Delta CMRO_2$. Our interpretation of the results assumes that $\Delta CMRO_2$ reflects

alterations in neural activity. There is some evidence that metabolic demand of evoked neural activity might be met by glucose metabolism (e.g. Raichle and Mintun 2006). We note that the rate of glucose consumption (CMRglu) is usually coupled to oxygen metabolic rate. Therefore, we expect that the CMRglu changes (ΔCMRglu) in our experiment would be similar to the measured $\Delta CMRO_2$. Furthermore, the time that $\Delta CMRO_2$ and ΔCMRglu are most likely to be decoupled is during the first several seconds after stimulation onset (prior to CBF response). Because we used a block design with stimulus durations of at least 20 s, we consider $\Delta CMRO_2$ measurement as an accurate reflection of ΔCMRglu and neural activity (cf. Lin et al. 2010).

Variance between studies comparing the cerebrovascular characteristics of younger and older adults (Ross et al. 1997; Taoka et al. 1998; D'Esposito et al. 1999; Huettel et al. 2001; Restom et al. 2007; Ances et al. 2009; Lu et al. 2011) suggest that age differences in the BOLD response arise from a complex and variable relationship between ΔCBF and $\Delta CMRO_2$ such that ΔCBF increases lead to BOLD amplitude increases whereas $\Delta CMRO_2$ increases lead to BOLD amplitude decreases (Buxton et al. 2004). The present results, showing age-related $\Delta CBF/\Delta CMRO_2$ alterations in primary visual regions, suggest that prior results might be more consistent than previously thought.

In regions where age-related changes in ΔCBF and $\Delta CMRO_2$ occur (Heo et al. 2010; Chen et al. 2011; Lu et al. 2011), the $\Delta CBF/\Delta CMRO_2$ ratio could differ substantially between younger and older groups leading to apparent age differences, or changes in one factor could offset changes in the other factor leading to apparent age-equivalence. For example, age-equivalent BOLD signal has been observed in medial temporal lobe in numerous studies (e.g. Morcom et al. 2003; Persson et al. 2011), even in the presence of ΔCBF increases (Restom et al. 2007). Our results support the conclusion that these results are more a reflection of age-related increases in $\Delta CMRO_2$, minimized by the effects of increased ΔCBF, than age-equivalence in neural activity per se (cf. Restom et al. 2007). In contrast to results in medial temporal lobe, our results show that the visual-cortex $\Delta CBF/\Delta CMRO_2$ ratio diminishes with age due to age-differential increases in $\Delta CMRO_2$, with age-equivalence in ΔCBF leading to decreases in BOLD responding in older compared with younger groups (cf. Ross et al. 1997). Such cross-cortex variability (Rypma and D'Esposito 2001; Rypma et al. 2006; Rypma and Prabhakaran 2009) has important implications for neurocognitive aging hypotheses based on BOLD signal because it suggests that regional BOLD age-differences, or age-equivalence, cannot be unambiguously interpreted in terms of neural activity.

Regional variation in $\Delta CBF/\Delta CMRO_2$ might also mediate disease-related BOLD signal change. For example, in schizophrenia there is a significant shift in BOLD signal patterns across cortex compared with controls that is correlated with performance declines (Callicott et al. 2000; Winterer et al. 2006; Yoon et al. 2008). Winterer et al. (2006), for instance, observed that the prefrontal BOLD signal of schizophrenic patients was more diffuse, more variable, and less organized than that of healthy individuals, and these indices were related to slower RTs.

Likewise, cognitive training results in regional BOLD signal variation in healthy samples that might indicate experience-related shifts in $\Delta CBF/\Delta CMRO_2$. Specifically, cross-cortical BOLD signal decreases over time with practice. This pattern suggests that task-specific knowledge might be focused across many brain regions for initial, effortful, task execution, and learning, but is then streamlined for skilled task execution (Petersen et al. 1998). Poldrack et al. (1998) observed BOLD signal decreases and increases across differing cortical regions with both skill learning and item-specific learning. Seger et al. (2000) also found learning-related shifts in BOLD signal patterns, from mainly right-hemisphere early in learning to bilateral BOLD signal later in learning. Thus, it might be that cortical variations in $\Delta CBF/\Delta CMRO_2$ could change over cortical regions, reflecting intervening processes of age, disease, learning, and other influences.

Our results further suggest intriguing relationships between variation of ΔCBF, $\Delta CMRO_2$, and behavior. The associations we observed between age-related performance reductions and reductions in the $\Delta CBF/\Delta CMRO_2$ ratio support the hypothesis that increased oxygen demand in the aging neural apparatus, not accommodated by vascular activity, is the basis for reduced functional efficiency at the neural level and reduced processing efficiency at the cognitive level (assuming no $CMRO_2$-baseline induced bias). While further research is required, these results provide important clues to the link between the neurophysiologic changes, and the pervasive behavioral changes, that accompany human aging.

Funding

This work was supported by the National Institutes of Health (1R01AG029523 [to B.R.] and R01MH084021 [to H.L.]). Funding to pay the Open Access publication charges for this article was provided by the National Institute of Health (1R01AG029523 [to B.R.]).

Notes

The authors wish to thank Andrew Hillis, Lee Jordan, Mary Jo Maciejewski, Traci Sandoval, Rani Varghese, Feng Xu, and Uma Yezhuvath for their assistance with various aspects of data collection and processing, and Lars Bäckman and Hervé Abdi for comments on an earlier draft of this manuscript. We thank John Wiley and Sons for permission to reprint and modify Hoge et al.'s (1999a) Figure 1*b* from their *Magnetic Resonance in Medicine* publication (Fig. 1). *Conflict of Interest*: The authors have no conflicts of interest to declare.

References

Ances BM, Liang CL, Leontiev O, Perthen JE, Fleisher AS, Lansing AE, Buxton RB. 2009. Effects of aging on cerebral blood flow, oxygen metabolism, and blood oxygenation level dependent responses to visual stimulation. Hum Brain Mapp. 30:1120–1132.

Anders TR, Fozard JL, Lillyquist TD. 1972. Effects of age upon retrieval from short-term memory. Dev Psychol. 6:214–217.

Aslan S, Xu F, Wang PL, Uh J, Yezhuvath US, van Osch M, Lu H. 2010. Estimation of labeling efficiency in pseudocontinuous arterial spin labeling. Magn Reson Med. 63:765–771.

Benjamini Y, Hochberg Y. 2000. On the adaptive control of the false discovery rate in multiple testing with independent statistics. J Educ Behav Stat. 25:60–83.

Boumezbeur F, Mason GF, de Graff RA, Behar KL, Cline GW, Shulman GI, Rothman DL, Petersen KF. 2010. Altered brain mitochondrial metabolism in healthy aging as assessed by *in vivo*

magnetic resonance spectroscopy. J Cereb Blood Flow Metab. 30:211–221.
Brant-Zawadzki M, Gillan GD, Nitz WR. 1992. MP RAGE: a three dimensional, T1-weighted, gradient-echo sequence—initial experience in the brain. Radiology. 182:769–775.
Brodmann K. 2006/1909. Brodmann's localization in the cerebral cortex: the principles of comparative localization in the cerebral cortex based on cytoarchitectonics. Garey LJ, translator. New York: Springer.
Brown GG, Perthen JE, Liu TT, Buxton RB. 2007. A primer on functional magnetic resonance imaging. Neuropsychol Rev. 17:107–125.
Buxton RB, Frank LR. 1997. A model for the coupling between cerebral blood flow and oxygen metabolism during stimulation. J Cereb Blood Flow Metab. 17:64–72.
Buxton RB, Uludag K, Dubowitz DJ, Liu TT. 2004. Modeling the hemodynamic response to brain activation. Neuroimage. 23: S220–S233.
Cabeza R. 2002. Hemispheric asymmetry reduction in older adults: the HAROLD model. Psychol Aging. 17:85–100.
Callicott JH, Bertolino A, Mattay VS, Langheim FJP, Duyn J, Coppola R, Goldberg TE, Weinberger DR. 2000. Physiological dysfunction of the dorsolateral prefrontal cortex in schizophrenia revisited. Cereb Cortex. 10:1092–1978.
Cauli B, Hamel E. 2010. Revisiting the role of neurons in neurovascular coupling. Front Neuroenergetics. 2:9.
Chen JJ, Rosas HD, Salat DH. 2011. Age-associated reductions in cerebral blood flow are independent from regional atrophy. Neuroimage. 55:468–478.
Chiarelli PA, Bulte DP, Piechnik S, Jezzard P. 2007. Sources of systematic bias in hypercapnia-calibrated functional MRI estimation of oxygen metabolism. Neuroimage. 34:35–43.
Cox RW. 1996. AFNI: software for analysis and visualization of functional magnetic resonance neuroimages. Comput Biomed Res. 29:162–173.
Craik FIM, Jennings JM. 1992. Human memory. In: Craik FIM, Salthouse TA, editors. The handbook of aging and cognition. Hillsdale (NJ): Lawrence Erlbaum Associates. p 51–110.
Davis TL, Kwong KK, Weisskoff RM, Rosen BR. 1998. Calibrated functional MRI: mapping the dynamics of oxidative metabolism. Proc Natl Acad Sci USA. 95:1834–1839.
de Jager CA, Hogervorst E, Combrinck M, Budge MM. 2003. Sensitivity and specificity of neuropsychological tests for mild cognitive impairment and Alzheimer's disease. Psychol Med. 33:1039–1050.
D'Esposito M, Deouell LY, Gazzaley A. 2003. Alterations in the BOLD fMRI signal with ageing and disease: a challenge for neuroimaging. Nat Rev Neurosci. 4:863–872.
D'Esposito M, Zarahn E, Aguirre GK, Rypma B. 1999. The effect of normal aging on the coupling of neural activity to the BOLD hemodynamic response. Neuroimage. 10:6–14.
Folstein MF, Folstein SE, McHugh PR. 1975. 'Mini-Mental State': a practical method for grading the cognitive state of patients for the clinician. J Psychiatr Res. 12:189–198.
Garcia DM, de Bazelaire C, Alsop D. 2005. Pseudo-continuous flow driven adiabatic inversion for arterial spin labeling. Proc Int Soc Magn Reson Med. 13:37.
Gjedde A. 1997. The relation between brain function and cerebral blood flow and metabolism. Philadelphia, PA: Lippincott-Raven Publishers.
Gössl C, Fahrmeir L, Auer DP. 2001. Bayesian modeling of the hemodynamic response function in BOLD fMRI. Neuroimage. 14:140–148.
Grady CL. 2002. Age-related differences in face processing: a meta-analysis of three functional neuroimaging experiments. Can J Exp Psychol. 56:208–220.
Grubb RL, Raichle ME, Eichling JO, Ter-Pogossian MM. 1974. The effects of changes in $PaCO_2$ on cerebral blood volume blood flow and vascular mean transit time. Stroke. 5:630–639.
Hasher L, Zacks RT. 1988. Working memory comprehension and aging: a review and a new view. In: Bower GH, editor. The psychology of learning and motivation: advances in research and theory, Vol 22. San Diego (CA): Academic Press. p 193–225.
Hedden T, Gabrieli JDE. 2004. Insights into the ageing mind: a view from cognitive neuroscience. Nat Rev Neurosci. 5:87–96.
Heo S, Prakash RS, Voss MW, Erickson KI, Ouyang C, Sutton BP, Kramer AF. 2010. Resting hippocampal blood flow, spatial memory and aging. Brain Res. 1315:119–127.
Hoge RD, Atkinson J, Gill B, Crelier GR, Marrett S, Pike GB. 1999a. Investigation of BOLD signal dependence on cerebral blood flow and oxygen consumption: the deoxyhemoglobin dilution model. Magn Reson Med. 42:849–863.
Hoge RD, Atkinson J, Gill B, Crelier GR, Marrett S, Pike GB. 1999b. Linear coupling between cerebral blood flow and oxygen consumption in activated human cortex. Proc Natl Acad Sci USA. 96:9403–9408.
Huettel SA, Singerman JD, McCarthy G. 2001. The effects of aging upon the hemodynamic response measured by functional MRI. Neuroimage. 13:161–175.
Hyder F, Kida I, Behar KL, Kennan RP, Maciejewski PK, Rothman DL. 2001. Quantitative functional imaging of the brain: towards mapping neuronal activity by BOLD fMRI. NMR Biomed. 14:413–431.
Hyder F, Rothman DL, Shulman RD. 2002. Total neuroenergetics support localized brain activity: implications for the interpretation of fMRI. Proc Natl Acad Sci USA. 99:10771–10776.
Iadecola C. 2004. Neurovascular regulation in the normal brain and in Alzheimer's disease. Nat Rev Neurosci. 5:347–360.
Keppel G, Wickens TD. 2004. Simultaneous comparisons and the control of type I errors. In: Design and analysis: A researcher's handbook. 4th ed. Upper Saddle River (NJ): Pearson Prentice Hall. p 111–130.
Kety SS. 1956. Human cerebral blood flow and oxygen consumption as related to aging. J Chronic Dis. 3:478–486.
Leontiev O, Buxton RB. 2007. Reproducibility of BOLD perfusion and $CMRO_2$ measurements with calibrated-BOLD fMRI. Neuroimage. 35:175–184.
Leontiev O, Dubowitz DJ, Buxton RB. 2007. $CBF/CMRO_2$ coupling measured with calibrated-BOLD fMRI: sources of bias. Neuroimage. 36:1110–1122.
Lin A-L, Fox PT, Hardies J, Duong TQ, Gao J-H. 2010. Nonlinear coupling between cerebral blood flow, oxygen consumption, and ATP production in visual cortex. Proc Natl Acad Sci USA. 107:8446–8451.
Lu H, van Zijl PCM. 2005. Experimental measurement of parenchymal BOLD effects and tissue oxygen extraction fractions using multi-echo vassal fMRI at 1.5 and 3.0 T. Magn Reson Med. 53:808–816.
Lu H, Xu F, Rodrigue KM, Kennedy KM, Cheng Y, Flicker B, Hebrank AC, Uh J, Park DC. 2011. Alterations in cerebral metabolic rate and blood supply across the adult lifespan. Cereb Cortex. 21:1426–1434.
Marchal G, Rioux P, Petit-Taboue MC, Sette G, Travere JM, Le Poec C, Courtheoux P, Derlon JM, Baron JC. 1992. Regional cerebral oxygen consumption, blood flow, and blood volume in healthy human aging. Arch Neurol. 49:1013–1020.
Moeller JR, Ishikawa T, Dhawan V, Spetsieris P, Mandel F, Alexander GE, Grady C, Pietrini P, Eidelberg D. 1996. The metabolic topography of normal aging. J Cereb Blood Flow Metab. 16:385–398.
Mohtasib RS, Lumley G, Goodwin JA, Emsley HCA, Slumig V, Parkes LM. 2012. Calibrated fMRI during a cognitive Stroop task reveals reduced metabolic response with increasing age. Neuroimage. 59:1143–1151.
Morcom AM, Good CD, Frackowiak RSJ, Rugg MD. 2003. Age effects on the neural correlates of successful memory encoding. Brain. 126:213–229.
Motes MA, Biswal BB, Rypma B. 2010. Age-dependent relationships between prefrontal cortex activation and processing efficiency. Cogn Neurosci. 2:1–10.
Nyberg L, Bäckman L. 2011. Memory changes and the aging brain: a multimodal imaging approach. In Schaie KW, Willis SL, editors. Handbook of the Psychology of Aging. San Diego (CA): Academic Press. p 121–132.
Ogawa S, Lee TM. 1990. Magnetic resonance imaging of blood vessels at high fields: *in vivo* and *in vitro* measurements and image simulation. Magn Reson Med. 16:9–18.

Ogawa S, Tank DW, Menon R, Ellermann JM, Kim S-G, Merkle H, Ugurbil K. 1992. Intrinsic signal changes accompanying sensory stimulation: functional brain mapping with magnetic resonance imaging. Proc Natl Acad Sci USA. 89:5951–5955.

Park DC, Lautenschlager G, Hedden T, Davidson NS, Smith AD, Smith PK. 2002. Models of visuospatial and verbal memory across the adult life span. Psychol Aging. 17:299–320.

Pasley BN, Inglis BA, Freeman RD. 2007. Analysis of oxygen metabolism implies a neural origin for the negative BOLD response in human visual cortex. Neuroimage. 36:269–276.

Persson J, Kalpouzos G, Nilsson L-G, Ryberg M, Nyberg L. 2011. Preserved hippocampus activation in normal aging as revealed by fMRI. Hippocampus. 21:753–766.

Petersen SE, van Mier H, Fiez JA, Raichle ME. 1998. The effects of practice on the functional anatomy of task performance. Proc Natl Acad Sci USA. 95:853–860.

Poldrack R, Desmond J, Glover G, Gabrieli J. 1998. The neural basis of visual skill learning: an fMRI study of mirror reading. Cereb Cortex. 8:1–10.

Poline J-B, Strother SC, Dehaene-Lamberta G, Egan GF, Lancaster JL. 2006. Motivation and synthesis of the FIAC experiment: reproducibility of fMRI results across expert analyses. Hum Brain Mapp. 27:351–359.

Raichle ME, Mintun MA. 2006. Brain work and brain imaging. Annu Rev Neurosci. 29:449–476.

Rajah MN, D'Esposito M. 2005. Region-specific changes in prefrontal function with age: a review of PET and fMRI studies on working and episodic memory. Brain. 128:1964–1983.

Restom K, Bangen KJ, Bondi MW, Perthen JE, Liu TT. 2007. Cerebral blood flow and BOLD responses to a memory encoding task: a comparison between healthy young and elderly adults. Neuroimage. 37:430–439.

Reuter-Lorenz PA, Cappell KA. 2008. Neurocognitive aging and the compensation hypothesis. Curr Dir Psychol Sci. 17:177–182.

Ross MH, Yurgelun-Todd DA, Renshaw PF, Maas LC, Mendelson JH, Mello NK, Cohen BM, Levin JM. 1997. Age-related reduction in functional MRI response to photic stimulation. Neurology. 48: 173–176.

Rossi DJ. 2006. Another BOLD role for astrocytes: coupling blood flow to neural activity. Nat Neurosci. 9:159–160.

Rypma B, Berger JS, Genova HM, Rebbechi D, D'Esposito M. 2005. Dissociating age-related changes in cognitive strategy and neural efficiency using event-related fMRI. Cortex. 41:582–594.

Rypma B, Berger JS, Prabhakaran V, Bly BM, Kimberg DY, Biswal BB, D'Esposito M. 2006. Neural correlates of cognitive efficiency. Neuroimage. 33:969–979.

Rypma B, D'Esposito M. 2000. Isolating the neural mechanisms of age-related changes in human working memory. Nat Neurosci. 3:509–515.

Rypma B, D'Esposito M. 2001. Age-related changes in brain-behavior relationships: evidence from event-related functional MRI studies. Eur J Cogn Psychol. 13:235–256.

Rypma B, Prabhakaran V. 2009. When less is more and when more is more: the mediating roles of capacity and speed in brain-behavior efficiency. Intelligence. 37:207–222.

Salthouse TA. 1996. The processing-speed theory of adult age differences in cognition. Psychol Rev. 103:403–428.

Seger CA, Poldrack RA, Prabhakaran V, Zhao M, Glover GH, Gabrieli JDE. 2000. Hemispheric asymmetries and individual differences in visual concept learning as measured by functional MRI. Neuropsychologia. 38:1316–1324.

Speranza F, Moraglia G, Schneider BA. 2001. Binocular detection of masked patterns in young and old observers. Psychol Aging. 16:281–292.

Stefanovic B, Warnking JM, Pike GB. 2004. Hemodynamic and metabolic responses to neuronal inhibition. Neuroimage. 22:771–778.

Takano T, Tian G-F, Peng W, Lou N, Libionka W, Han X, Nedergaard M. 2006. Astrocyte-mediated control of cerebral blood flow. Nat Neurosci. 9:260–267.

Taoka T, Iwasaki S, Uchida H, Fukusumi A, Nakagawa H, Kichikawa K, Takayama K, Yoshioka T, Takewa M, Ohishi H. 1998. Age correlation of the time lag in signal change on EPI-fMRI. J Comput Assist Tomog. 22:514–517.

Van Essen DC. 2005. A Population-Average, Landmark- and Surface-based (PALS) atlas of human cerebral cortex. Neuroimage. 28:635–662.

Van Essen DC, Drury HA, Dickson J, Harwell J, Hanlon D, Anderson CH. 2001. An integrated software suite for surface-based analyses of cerebral cortex. J Am Med Inform Assoc. 8:443–459.

Welford AT. 1981. Signal noise performance and age. Hum Factors. 23:97–109.

Winterer G, Musso F, Weinberger DR, Beckmann C, Mattay V, Egan MF, Jones DW, Callicott JH, Coppola R. 2006. Instability of prefrontal signal processing in schizophrenia. Am J Psychiatr. 163:1960–1968.

Wong EC, Luh W-M, Liu TT. 2000. Turbo ASL: arterial spin labeling with higher SNR and temporal resolution. Magn Reson Med. 44:511–515.

Yoon J, Tamir D, Minzenberg M, Ragland J, Ursu S, Carter C. 2008. Multivariate pattern analysis of functional magnetic resonance imaging data reveals deficits in distributed representations in schizophrenia. Biol Psychiatr. 64:1035–1041.